

Bazant, Z.P., Tabbara, M.R., Kazemi, M.T., and Pijaudier-Cabot, G. (1990). "Random particle simulation of damage and fracture in particulate or fiber-reinforced composites", *Damage Mechanics in Engineering Materials* (ASME Winter Annual Meeting, Dallas, Nov. 1990), AMD-Vol.109, ed. by J. W. Ju, D. Krajcinovic, and H. L. Schreyer, Am. Soc. of Mechanical Engrs., 41-55.

# DAMAGE MECHANICS IN ENGINEERING MATERIALS

PRESENTED AT  
THE WINTER ANNUAL MEETING OF  
THE AMERICAN SOCIETY OF MECHANICAL ENGINEERS  
DALLAS, TEXAS  
NOVEMBER 25-30, 1990

SPONSORED BY  
THE APPLIED MECHANICS DIVISION AND  
THE MATERIALS DIVISION, ASME

EDITED BY  
J. W. JU  
PRINCETON UNIVERSITY

D. KRAJCINOVIC  
ARIZONA STATE UNIVERSITY

H. L. SCHREYER  
UNIVERSITY OF NEW MEXICO

THE AMERICAN SOCIETY OF MECHANICAL ENGINEERS

345 East 47th Street • United Engineering Center • New York, NY 10017

## RANDOM PARTICLE SIMULATION OF DAMAGE AND FRACTURE IN PARTICULATE OR FIBER-REINFORCED COMPOSITES

Zdenek P. Bazant, Mazen R. Tabbara, Mohammad T. Kazemi, and Gilles Pijaudier-Cabot

Center for Advanced Cement-Based Materials  
Northwestern University  
Evanston, Illinois

### ABSTRACT

Presented is a particle model for brittle aggregate composite materials such as concretes, rocks or ceramics. The model is also applicable to the behavior of unidirectionally reinforced fiber composites in the transverse plane. A method of random computer generation of the particle system meeting the prescribed particle size distribution is presented. The particles are assumed to be elastic and have only axial interactions, as in a truss. The interparticle contact layers of the matrix are described by a softening stress-strain relation corresponding to a prescribed microscopic interparticle fracture energy. Both two- and three-dimensional versions of the model are easy to program, but the latter poses, at present, forbidding demands for computer time. The model is shown to realistically simulate the spread of cracking and its localization. Furthermore, the model exhibits a size effect on: (1) the nominal strength, agreeing with the previously proposed size effect law, and (2) the slope of the post-peak load-deflection diagrams of specimens of different sizes. For direct tensile specimens, the model predicts development of asymmetric response after the peak load.

### INTRODUCTION

It is now generally accepted that inelastic deformation and fracture of brittle heterogeneous materials such as concrete or fiber composites can be adequately modeled neither by classical (local) continuum material models nor by linear elastic fracture mechanics. Although nonlinear fracture models and nonlocal continuum models can no doubt go a long way towards a realistic description, they are inherently incapable of capturing those phenomena which are strongly affected by the randomness of material heterogeneity on the microscale and are localized to a small but non-negligible region. The continuum models can describe well the mean of the macroscopic material response but not its variance. Even when generalizations such as the stochastic finite element method are considered, the assumed spatial randomness can only be correct in the overall sense and cannot capture the effect of random local material inhomogeneities on the localization of damage and failure. It is for these reasons that a direct simulation of the random microstructure of these materials is useful. As demonstrated by Zubelewicz and Bazant (1987), a model simulating the microstructure can describe progressive

distributed microcracking with gradual softening and with a large cracking zone (large relative to the aggregate size).

The present paper summarizes the results of a study which will be reported in detail elsewhere (Bažant et al., 1990). The principal objective of this study has been to determine the effect of the size of the specimen or structure on the maximum load, the subsequent softening behavior, and the spread of the microcracking zone. These are the key questions of fracture modeling. The material will be modeled as a system of randomly configured circular particles. This model is intended to simulate the behavior of concrete, but can also be used for the behavior of unidirectionally reinforced fiber composites in the transverse plane, with microcracks parallel to the fibers and spreading in the transverse direction.

The present model is a modification and refinement of that recently developed by Zubelewicz and Bažant (1987). The idea of particle simulation is an older one; it was proposed by Cundall (1971), Serrano and Rodriguez-Ortiz (1973) and Kawai (1980). These models, which dealt with rigid particles which interact by friction and simulate the behavior of granular solids such as sand, were developed and extensively applied by Cundall (1978) and Cundall and Strack (1979), who called it the distinct element method. An extension of Cundall's method to the study of microstructure and crack growth in geomaterials with finite interfacial tensile strength was introduced by Zubelewicz and Mróz (1983), and Plesha and Alfantis (1983).

In the present model we neglect the shear and bending interaction of neighboring particles throughout their contact layers. With such a simplification the present model becomes similar to the random truss model of Burt and Dougill (1977). These investigators verified that the truss model yields a realistic strain-softening curve but they studied neither the fracture mechanics nor size effect aspects, and their method of system generation was not based on the idea of particles with a prescribed gradation.

#### SUMMARY OF MATHEMATICAL FORMULATION

The adjacent circular or spherical particles shown in Fig. 1 are considered to interact only on the axial direction. Each strut connecting two adjacent particles consists of three segments simulating the aggregate particle and the interparticle contact layer. The two end segments, representing the particles, are assumed to be always elastic, with modulus  $E_a$ .

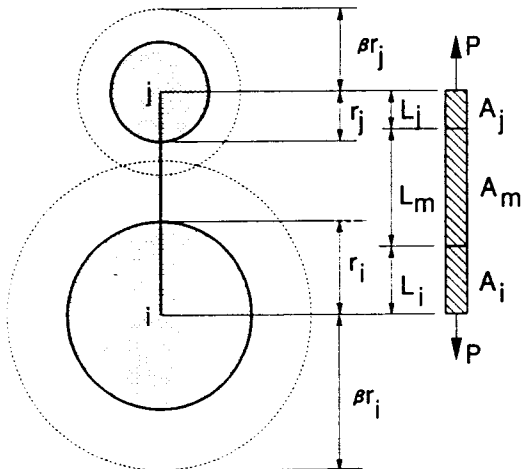


Fig. 1 Two adjacent circular particles with the corresponding truss member.

The central segment of the strut, representing the interparticle region of the matrix, is assumed to exhibit softening characterized by the triangular stress-strain relation shown in Fig. 2. The softening segment of the stress-strain relation varies so as to give the same stress-displacement relation regardless of the length of the central segment of the strut, thus assuring the fracture energy of this strut segment, represented by the area under the stress-displacement curve, to be constant.

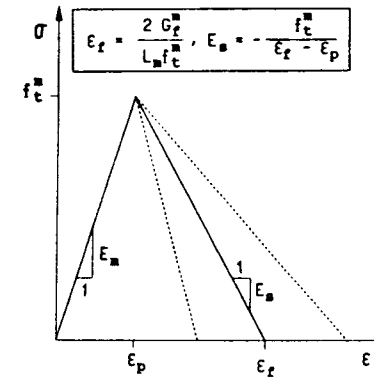


Fig. 2 Constitutive law for the matrix.

A simple method to generate the random particle system has been developed. The generation begins with the particles of the largest size, their coordinates are generated with a random number generator assuming a uniform probability density throughout the specimen area. For each generated location of the particle center, the program checks for possible overlaps with already generated particles, and the location is rejected if an overlap occurs. The random generation of particle locations then proceeds to the next smaller size, and the same procedure is repeated. The program continues until the last particle of the smallest size has been placed within the specimen.

The basic idea that makes the foregoing generation of the random particle system possible is that the particles are assumed to interact not only when they are in contact, but also when their influence regions overlap. These influence regions are assumed to be circles or spheres of a diameter which is  $\beta$ -times larger than the diameter of the particle (Fig. 1),  $\beta$  being an empirical constant ( $\beta=1.65$  has been used).

#### RESPONSE OF UNNOTCHED SPECIMENS

Geometrically similar specimens (Fig. 3) with depths = 3, 6 and 12 times the maximum particle size have been analyzed. The length of the specimens is always  $L = 8d/3$ . The diameters of the particles are 12, 8, 5, 3 and 1 mm, the volume ratio for each diameter is selected so as to model concrete. The response of the particle system can be solved by the same methods as used in nonlinear finite element analysis. The technique of incremental loading with iteration in each loading step has been applied to the equivalent truss mesh for each specimen. Fig. 4 shows such a mesh for a typical specimen.

#### Size Effect

A salient consequence of heterogeneity, which has fracture mechanics as well as probabilistic aspects, is the size effect on the failure load. If the failure is governed by criteria in terms of stress or strain (yield criteria), then geometrically similar specimens of different sizes must fail at the same value of the nominal stress at failure  $\sigma_u$ , defined as  $P_u/bd$ , where

$P_u$  = maximum load,  $d$  = depth of specimen, and  $b$  = thickness. To test this property, the specimens shown in Fig. 3 were subjected to prescribed uniform longitudinal displacement  $u$  at one end and restrained against displacements at the opposite end (Fig. 5). Displacement  $u$  has been incremented in small steps, and the axial force resultant  $P$  was calculated for the following material properties:  $G_f^m = 24 \text{ N/m}$ ,  $f_t^m = 3 \text{ MPa}$ ,  $E_m = 30 \text{ GPa}$ , and  $E_s = 6E_m$ . The diagrams

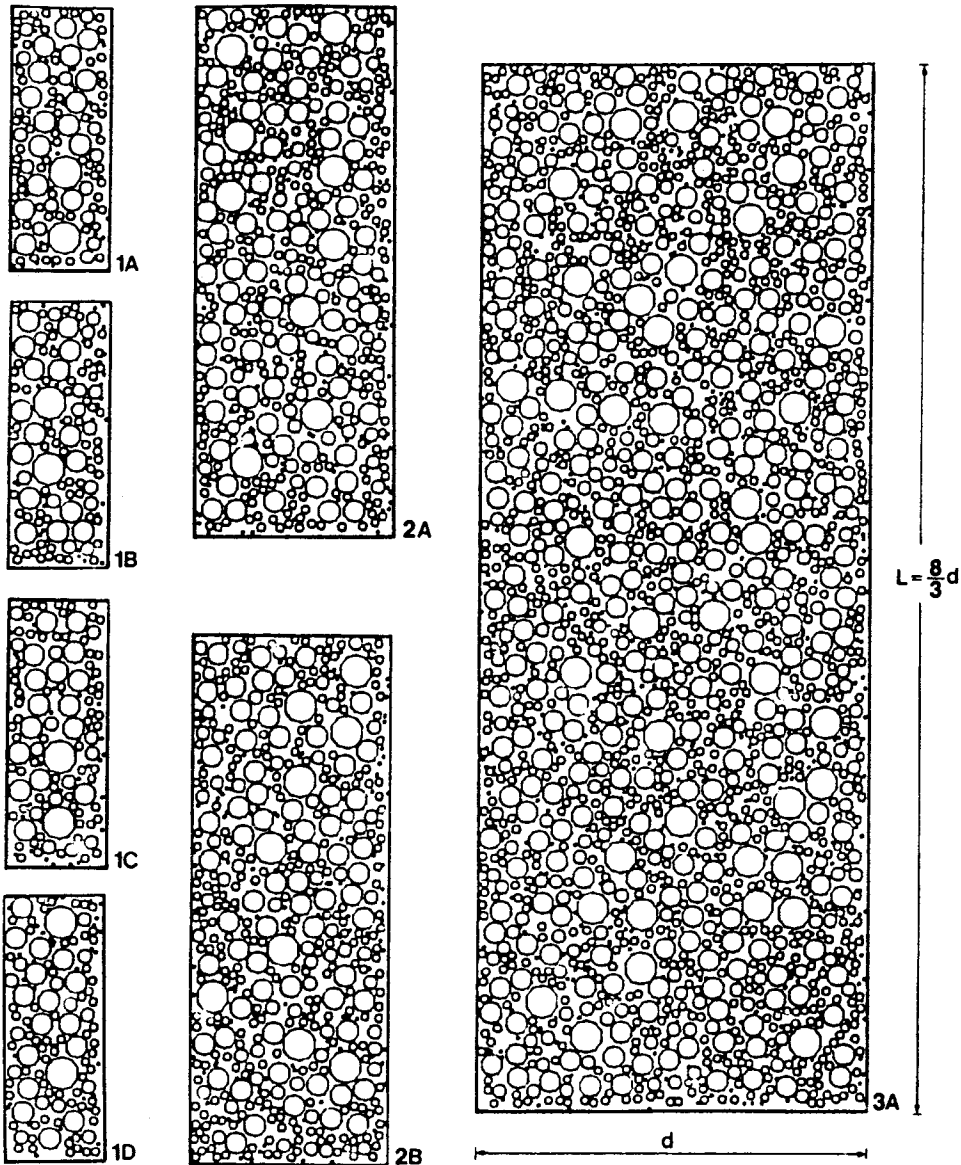


Fig. 3 Geometrically similar specimens of various sizes with randomly generated particles.

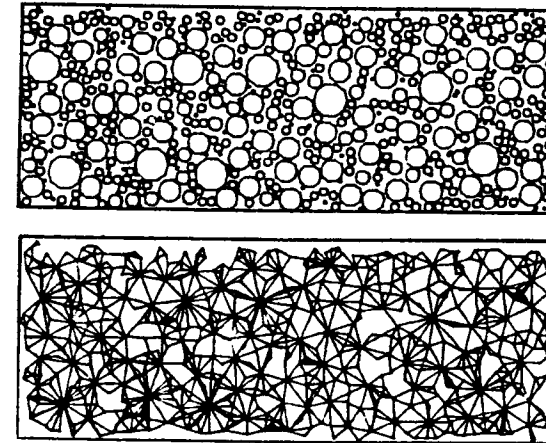


Fig. 4 A typical randomly generated specimen and its corresponding mesh of truss elements.

of load  $P$  versus load-point displacement  $u$  have been constructed; they are plotted in Fig. 6 for the small, medium and large specimens. Also shown are the load-deflection curves for specimens 1A, 2A and 3A scaled so that the peak point would coincide with (1,1). These curves reveal that the post-peak declining slope gets steeper as the specimen size increases.

The data points for maximum loads are plotted in Fig. 7 in terms of stress  $\sigma_m$  as a function of the specimen depth  $d$ . The nominal stress is normalized with respect to  $f_u$ , an arbitrary measure of material strength, taken here as  $f_u = f_t^m = 3 \text{ MPa}$ . The depth is normalized with respect to  $d_s$  = diameter of the largest particle = 12 mm. We see considerable scatter; therefore, the values of the nominal stress are averaged for each specimen size and are plotted as asterisks. These plots clearly reveal that there is a size effect.

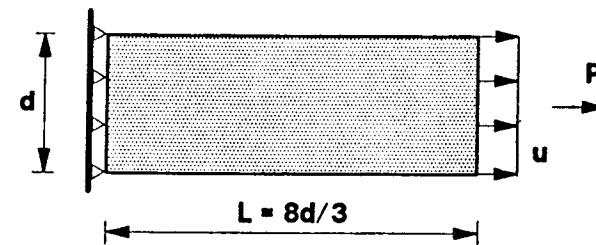


Fig. 5 Direct tension specimens with  $d = 36, 72$  and  $144 \text{ mm}$

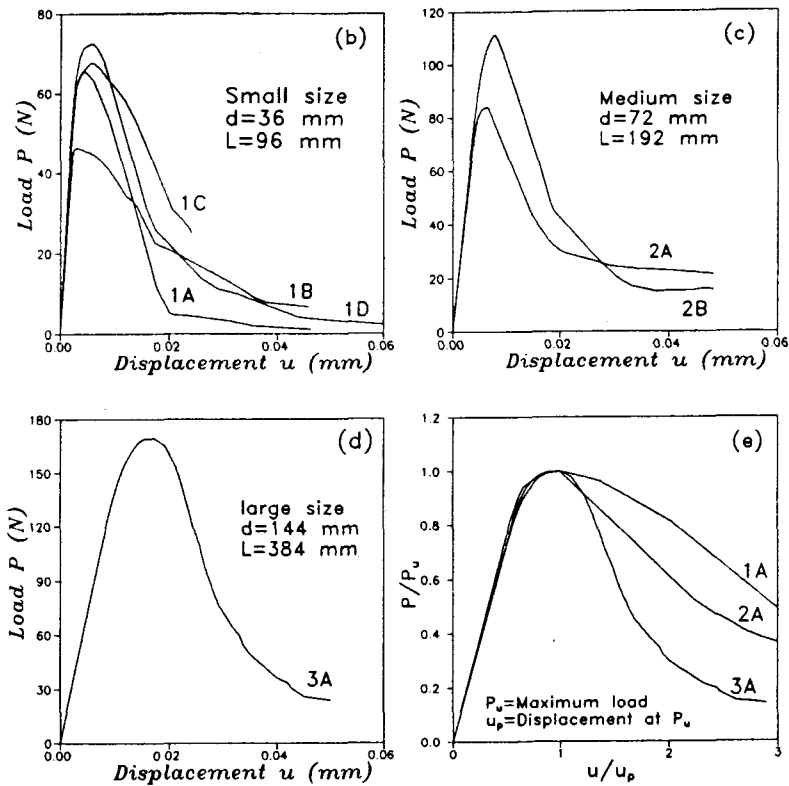


Fig. 6 Load displacement curves for (a) Small, (b) Medium, and (c) Large specimens; (e) normalized load-displacement curves.

The size effect for materials that exhibit progressive cracking is known to approximately follow the size effect equation proposed by Bažant (1984):

$$\sigma_N = \frac{Bf_u}{\sqrt{1 + d/d_0}} \quad (1)$$

where  $d_0 = \lambda_0 d_a$  and B,  $\lambda_0$  = empirical parameters. Eq. 1, which is approximate but usually applicable to size ranges up to 1:20, represents a gradual transition between the strength (or yield) criterion, for which there is no size effect on nominal strength, and linear elastic fracture mechanics, for which the size effect is the strongest possible ( $\sigma_N \propto d^{-1/2}$ ). For data fitting it is convenient to transform Eq. 1 to the linear regression plot  $Y = AX + C$ , in which  $X = d/d_0$ ,  $Y = (f_u/\sigma_N)^2$ ,  $C = 1/B^2$ , and  $A = C/\lambda_0$ .

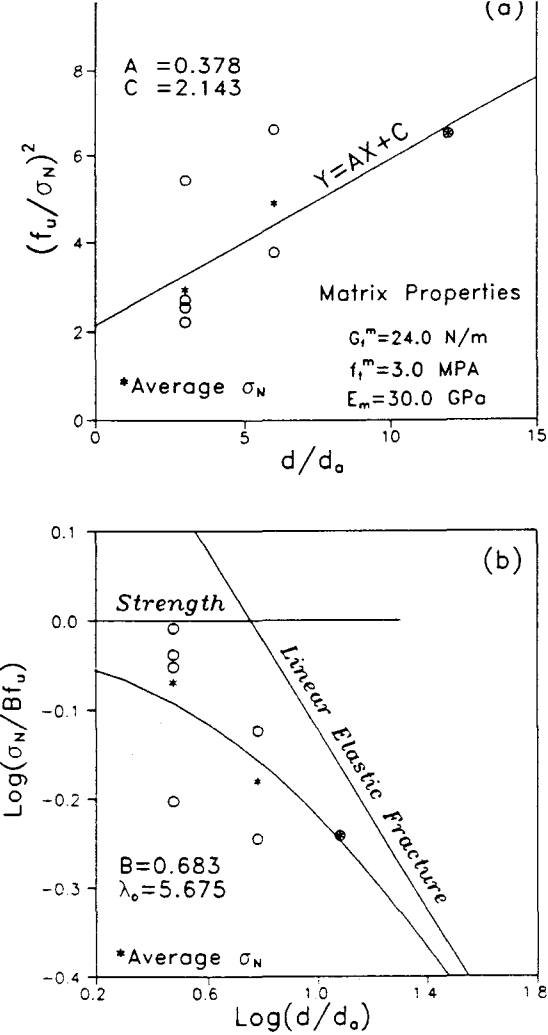


Fig. 7 Linear regression plot (a) and size effect plot (b) constructed from the maximum load values calculated for direct tension specimens of various sizes

For comparison, the lines representing the size effect according to the strength (or yield) criterion and according to the linear elastic fracture mechanics are also shown in Fig. 7b. From this it is evident that the size effect obtained is intermediate between the strength criterion and the linear elastic fracture mechanics. This may be expected on the basis of the fact that the specimens do not fail at cracking initiation but only after a crack band has already developed, in which case nonlinear fracture mechanics should be applicable.

#### Progressive Spread of Cracking

Fig. 8 shows for various specimens their microcrack patterns at the last calculated point on the load-deflection curve. Fig. 9 shows these patterns as

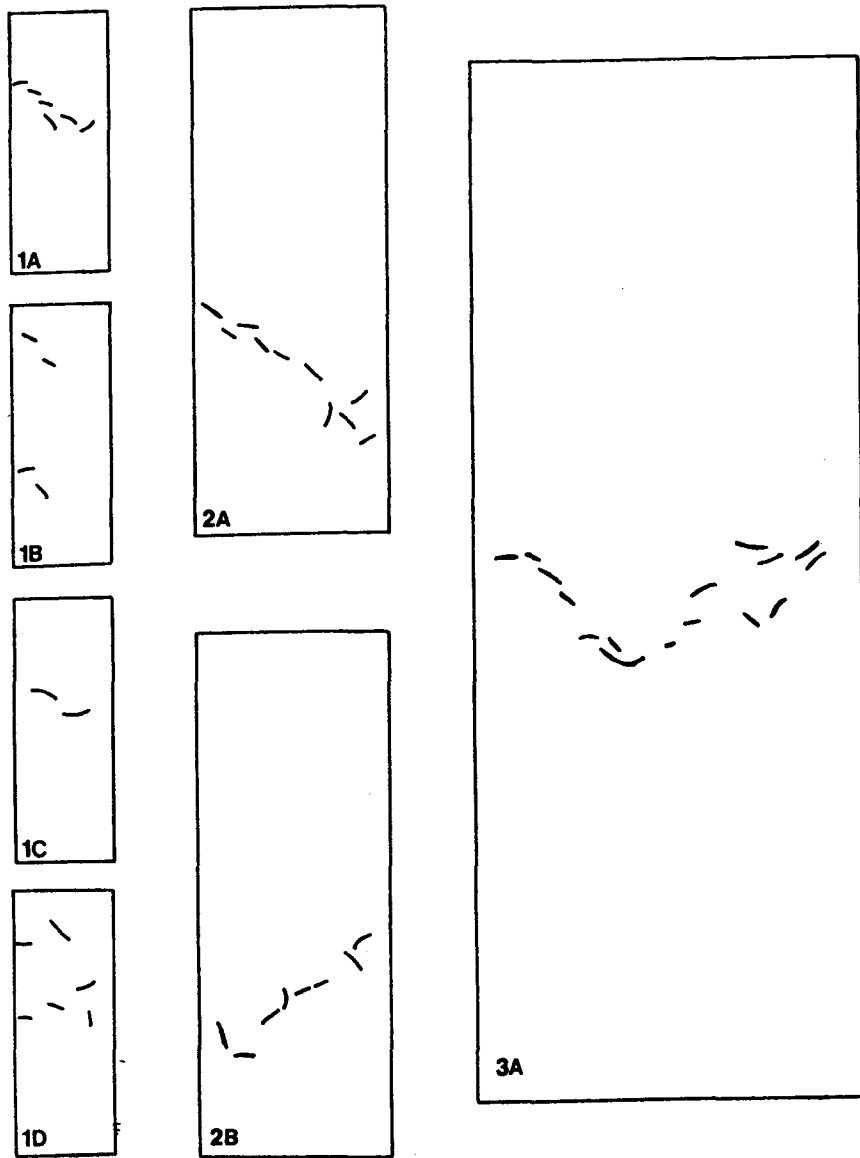


Fig. 8 Cracking patterns at the last calculated point on the load-displacement curve for unnotched specimens in tension.

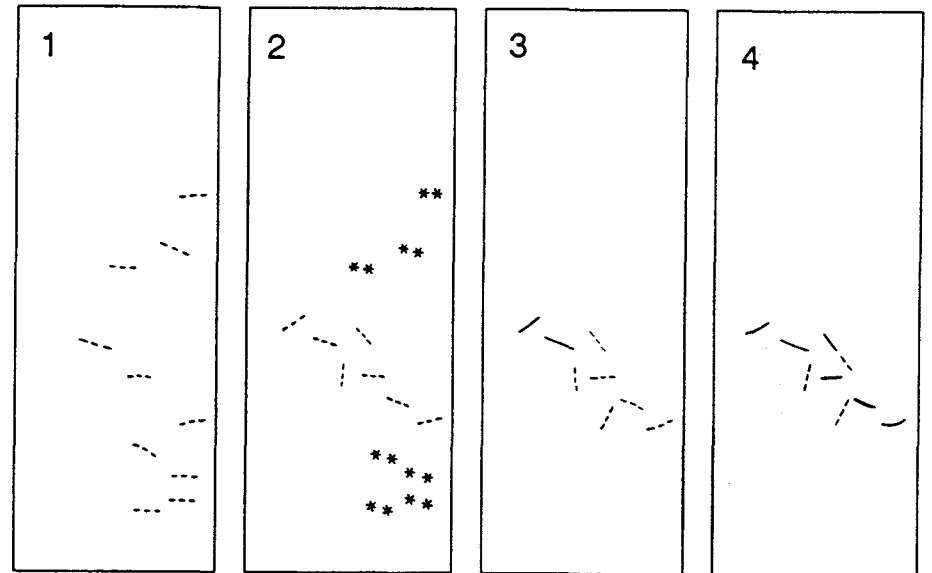
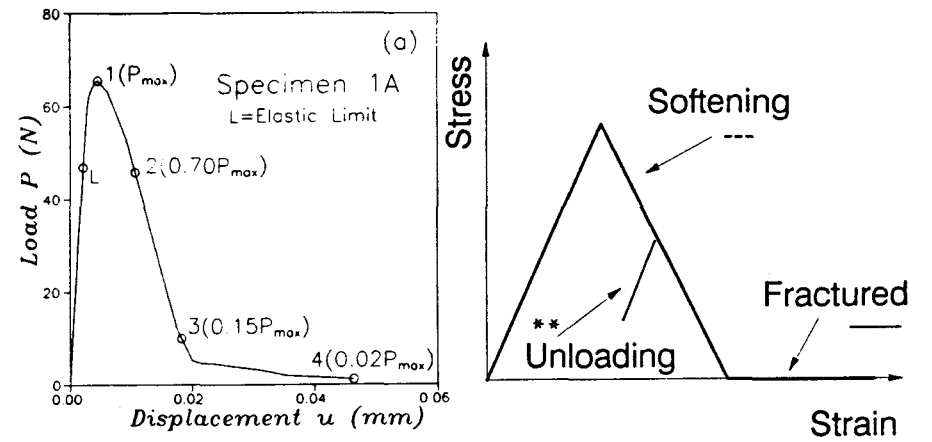


Fig. 9 Evolution of cracking with load level for specimen 1A

they develop in specimen 1A at various stages of loading corresponding to points 1, 2, 3 and 4. The fully formed and open cracks are shown by the solid lines, and the partially formed, developing (active) cracks which correspond to strain-softening states are shown by the dashed lines. Also shown are the previously formed cracks which are getting unloaded; these are represented by asterisks. We see that the cracks first start at many random locations throughout the specimen, but later many of these partially formed cracks unload, and only some of them, lying in a narrow transverse band, open further and lead to the final fracture.

#### Scatter of Stress Profile and Symmetry Breakdown

The distribution of the longitudinal component of the interparticle forces  $P_i$  throughout the cross section at distance  $x = 60$  mm from the fixed end is sketched, for specimen 1A, at various stages of loading in Fig. 10. We see that the nonuniformity in the distribution is getting more pronounced at later stages of loading. Furthermore, we see that the resultant of the longitudinal force tends to shift away from the center line, which indicates a tendency for these specimens to follow an asymmetric deformation pattern. The eccentricity,  $e$ , of the force resultant,  $P$ , is plotted as a function of  $P$  for two specimens (1A and 1B) in Fig. 11, in which the tendency towards an increasing eccentricity is clearly seen. A similar asymmetry was reported by Rots, Hordijk, and de Borst (1987) who studied by finite elements the evolution of crack bands in concrete tensile specimens.

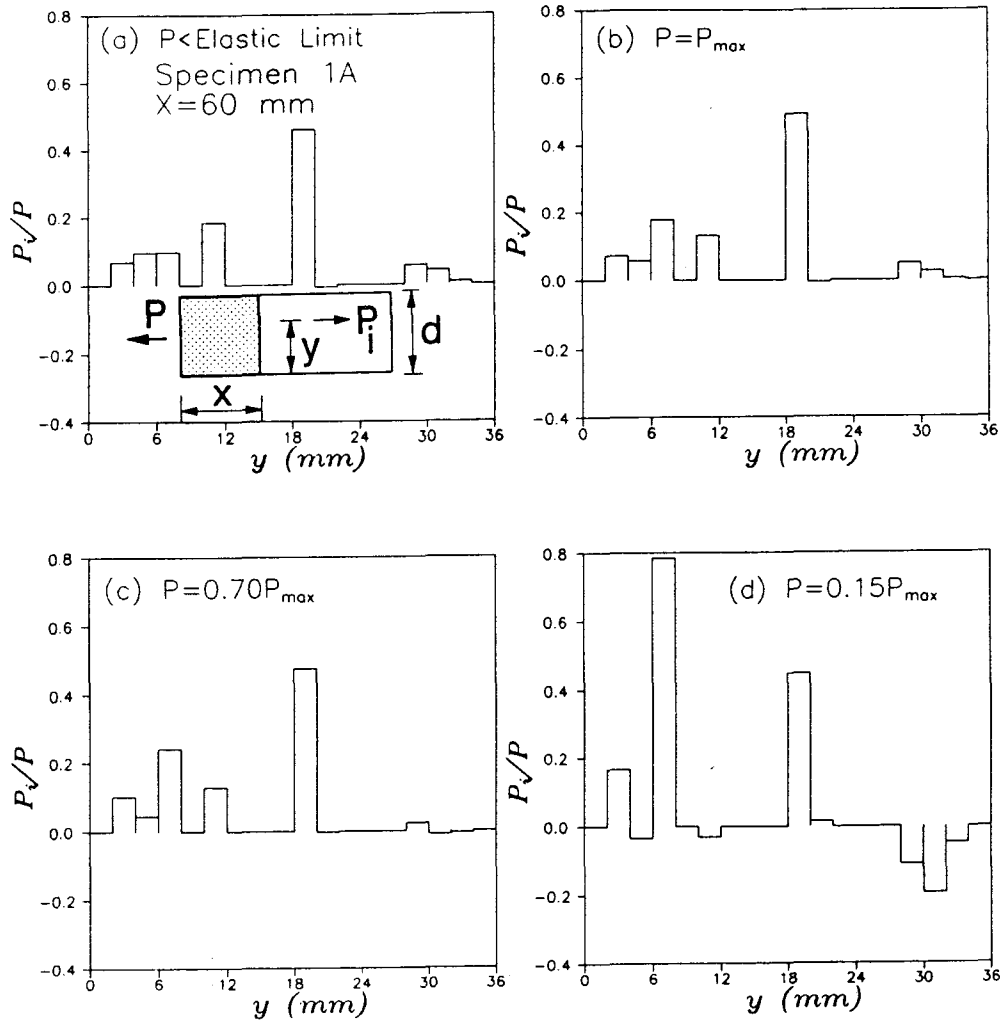


Fig. 10 Distribution of longitudinal component of interparticle forces throughout the cross section of specimen 1A.

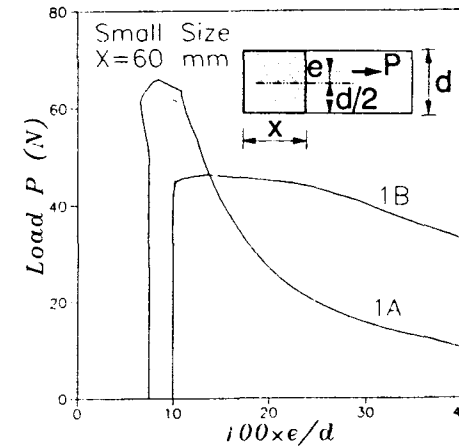


Fig. 11 Evolution of eccentricity as a function of load resultant.

#### Macroscopic Poisson's Ratio

To determine the Young's elastic modulus  $E$  and the macroscopic Poisson's ratio of the equivalent (smeared, homogenized) elastic continuum, the large specimen 3A was loaded in uniaxial tension by prescribing a very small uniform longitudinal displacement ( $u=0.004$ mm) at one end and restraining the specimen against displacement at the other end. Free sliding was allowed at the ends in the transverse direction. The displacements in the longitudinal direction,  $u_x$ , and the transverse direction,  $u_y$ , at the nodes with the maximum size aggregates were fitted by a linear field to determine the mean axial and lateral strains. To minimize the effect of boundary conditions, only nodes within an interior region ( $0.8d \times 0.8L$ ) were considered. For the mean uniaxial stress  $\sigma_x = 0.39$  MPa, the slope of the linear regression line for  $u_x$  as a function of the  $x$ -coordinate, which represents the mean (macroscopic) strain

in the x-direction, indicated the value  $\epsilon_x = 0.1154 \times 10^{-4}$ . From this,  $E = 3.4 \times 10^4$  MPa. A similar regression line gave the strain in the y-direction,  $\epsilon_y = -0.4234 \times 10^{-5}$ . The macroscopic Poisson ratio was then obtained as  $\nu = -\epsilon_y / \epsilon_x = 0.37$ . This value is close to the value of  $\nu = 1/3$ , which is the theoretical value for a very large two-dimensional random lattice that is statistically uniform and isotropic. Neither the calculated value  $\nu = 0.37$  nor the theoretical value  $\nu = 1/3$  for very large specimens is realistic for most particulate composites, including concrete, for which, typically,  $\nu = 0.18$ . The correct Poisson ratio of real particulate composites cannot be attained with the present model. The reason for this limitation is that only axial interactions between the particle centers are taken into account while shear stresses in the contact zones are neglected.

#### RESPONSE OF NOTCHED SPECIMENS

As we have seen, cracking in unnotched specimens that are initially stressed uniformly develops quite randomly. This prevents it to bring to light fracture properties of the particle system. To see these properties, notched specimens have also been simulated with the particle model. The notches were mathematically modeled by first generating the random particle configuration as if no notch existed, and then severing all the interparticle connections that cross the line of the mathematical notch depth,  $a_0 = d/6$  ( $\alpha_0 = a_0/d = 1/6$ ).

Fracture properties may be best determined by studying the size effect, since this effect represents the most important consequence of fracture mechanics. To this end, we analyze geometrically similar three-point-bend fracture specimens of three different sizes whose ratios are 1:2:4. Thus, three new specimens were generated as shown in Fig. 12.

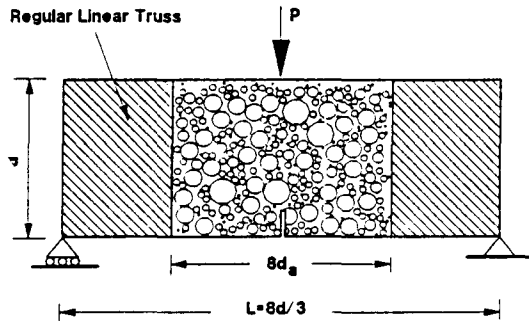


Fig. 12 Three-point-bend specimens with  $d = 36, 72$  and  $144$  mm

To save computer time, the truss modeling of the random particle system covered only the central region of the beam near the notch while the end portions of the specimen were modeled by a regular truss with linear elastic properties. This simplification has a negligible effect on the values of the maximum loads, as long as all the cracking occurs only outside the regular truss and far from its boundaries. Calculations verified that this was indeed the case. For the three-point-bend specimens, the random particle region width was taken to be equal to  $8d$  (96 mm) which coincided with the span of the smallest size specimen. Thus, no truss was added to a specimen of this size.

In the calculations of maximum loads, three different sets of matrix properties have been considered: (1)  $G_f^m = 24$  N/m,  $f_t^m = 3$  MPa, (2) 24 N/m, 1.5 MPa and (3) 240 N/m, 3 MPa with  $E_m = 30$  GPa and  $E_a = 6E_m$  for all cases. For each set, the regression line (plotted in Fig. 13a) yields the values of

slope A and intercept C, from which the values of B and  $\lambda_0$  follow; see Fig. 13b. The size effect curve according to Eq. 1 is also plotted, along with all the calculated points for the different sets of matrix properties. The results show a good agreement with Eq. 1. However, for the aforementioned values of material properties, the results are closer to linear elastic fracture mechanics than the test results obtained for similar specimens by Bažant and Pfeiffer (1987).

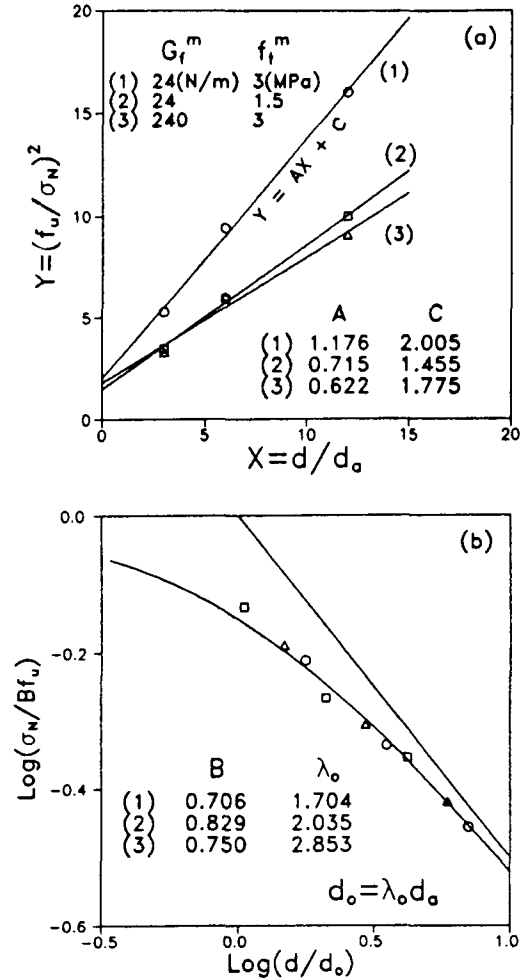


Fig. 13 Linear regression plot (a) and size effect plot (b) constructed from the maximum load values calculated for three-point-bend specimens of various sizes

From the size effect on the maximum loads, one can determine the fracture energy  $G_f$  of the idealized material represented by the random particle system, using the formula (Bažant and Pfeiffer, 1987)

$$G_f = \frac{g(\alpha_0)}{AE} f_u^2 d_a \quad (2)$$

Here  $E$  = Young's modulus (macroscopic), and  $g(\alpha_0)$  is the nondimensional energy

release rate according to linear elastic fracture mechanics;  $g(\alpha_0) = 6.07$  for the present specimens. One can also determine the size of the fracture process zone according to the formula (Bažant and Kazemi, 1988):

$$c_f = \frac{g(\alpha_0)}{g'(\alpha_0)} \lambda_0 d \quad (3)$$

where  $g'(\alpha_0)$  is the derivative of  $g(\alpha)$  which is evaluated at  $\alpha_0 = 1/6$ , and is equal to 35.2 for the present three-point-bend specimens.

Table 1 gives the values of  $G_f$  and  $c_f$  calculated for the three sets of matrix properties. Taking the properties in column (1) as reference, the results from column (2) show that a decrease of interparticle strength  $f_t^m$  will decrease  $G_f$  and increase  $c_f$ . However, the results from column (3) show that an increase of  $G_f^m$  will increase both  $G_f$  and  $c_f$ . Table 1 also includes the values obtained by Bažant and Kazemi (1988) from experiments on mortar and concrete. These values are in the same range as calculated here and could be matched even closer by adjusting the material properties of the model.

Three Point Bending	Particle Model			Experiment	
	(1)	(2)	(3)	Mortar	Concrete
$G_f$ (N/m)	16.5	6.8	31.2	20	37
$c_f$ (mm)	3.5	4.2	5.9	1.9	13.5

Table 1 Values of Fracture Energy  $G_f$  and Process Zone Size  $c_f$

## CONCLUSIONS

1. Random generation of a particle system with a given particle size distribution can be accomplished quite easily, due to the fact that the particles are circular (or spherical) and are not in contact but are separated by contact layers whose thickness is unspecified.

2. Modeling only the axial interactions of neighboring particles seems sufficient to obtain a realistic picture of the spread of cracking and fracture in concrete. The neglect of shear interactions might cause the fracture process zone to be shorter than the value reported from test on concrete specimens. However, the length of this zone can be increased by increasing the value of the interparticle fracture energy ( $G_f^m$ ) or by decreasing the value of the interparticle strength ( $f_t^m$ ).

3. The model can describe realistically the post-peak declining load-deflection diagram, which is predicted to get steeper as the specimen size increases.

4. In contrast to local continuum models, the present model is capable of describing the size effect on the nominal strength of unnotched specimens as well as notched specimens.

5. For direct tensile specimens, the model predicts development of asymmetric response after the peak load, such that the specimen bends and the axial force resultant becomes eccentric.

6. Some improvements of the model might be appropriate in: (1) determining the cross section areas of the truss members so as to make them dependent on the distance between particles, (2) controlling the Poisson's ratio without having to introduce shear interaction, (3) developing a method to connect the particle system in the cracking zone to a finite element mesh around this zone. This would significantly reduce the number of particles needed to analyze three-dimensional or large two-dimensional problems.

## ACKNOWLEDGEMENT

Partial financial support under AFSOR contract F49620-87-C-0030DEF with Northwestern University, monitored by Dr. Spencer T. Wu, is gratefully acknowledged. Support for preparing this paper was received from the Center for Advanced Cement-Based Materials at Northwestern University (NSF Grant DMR-8808432). Supercomputer time on CRAY (X-MP/48) was received from the National Center for Supercomputing Applications (NCSA) under grant number MSMB90006N.

## REFERENCES

- Bažant, Z. P. (1984). "Size effect in blunt fracture: concrete, rock, metal." *J. Engrg. Mech. Div., ASCE*, 110 (4), 518-535.
- Bažant, Z. P. and Pfeiffer, P. A. (1987) "Determination of fracture energy from size effect and brittleness number." *ACI Materials Journal*, 84 (6), 463-480
- Bažant, Z. P., and Kazemi, M.T. (1988). "Determination of fracture energy, process zone length and brittleness number from size effect, with application to rock and concrete." Report 88-7/498d Center for Concrete and Geomaterials, Northwestern University, Evanston, Illinois; also *International Journal of Fracture* (in press).
- Bažant, Z. P., Tabbara, M. R., Kazemi, M. T. and Pijaudier-Cabot G. (1990). "Random particle model for fracture of aggregate or fiber composites." *Journal of Engineering Mechanics Division, ASCE* (in press).
- Burt, N. J. and, Dougill, J. W. (1977). "Progressive failure in a model heterogeneous medium." *J. Engrg. Mech., ASCE*, 103 (3), 365-376
- Cundall, P. A. (1971). "A computer model for simulating progressive large scale movements in blocky rock systems." *Proc. Int. Symp. on Rock Fracture, ISRM, Nancy, France*, 2-8.
- Cundall, P. A. (1978). "BALL - A program to model granular media using the distinct element method." *Technical Note, Advanced Technology Group, Dames and Moore, London, England*.
- Cundall, P. A., and Strack, O. D. L. (1979). "A discrete numerical model for granular assemblies." *Geotechnique*, 29, 47-65.
- Kawai, T. (1980). "Some considerations on the finite element method." *Int. J. Numer. Meth. Engrg.*, 16, 81-120.
- Plesha, M. E., and Aifantis, E. C. (1983). "On the modeling of rocks with microstructure." *Proc. 24th U. S. Symp. on Rock Mechanics, Texas A&M Univ., College Station, Texas*, 27-39.
- Rots, J. G., Hordijk, D. A., and de Borst, R. (1987). "Numerical simulation of concrete fracture in direct tension." *Proc., 4th Int. Conf. on Numerical Methods in Fracture Mechanics, San Antonio, Texas, A.R. Luxmoore et al., eds., Pineridge Press, Swansea, U.K.*, 457-471.
- Serrano, A. A., and Rodriguez-Ortiz, J. M. (1973). "A contribution to the mechanics of heterogeneous granular media." *Proc., Symp. on Plasticity and Soil Mechanics, Cambridge, U.K.*
- Zubelewicz, A., and Bažant, Z. P. (1987). "Interface element modeling of fracture in aggregate composites." *J. Engrg. Mech. Div., ASCE*, 113 (11), 1619-1630.
- Zubelewicz, A., and Mróz, Z. (1983). "Numerical simulation of rock-burst processes treated as problems of dynamic instability." *Rock Mech. and Engrg.*, 16, 253-274.